EasyChair Preprint

№ 14582

Determine the Short Circuit Cutting Time of Fuse Cut Out for Energy Saving Amorphous Core Transformers

Bao Doan Thanh

August 28, 2024

2024 The 9th International Conference on Applying New Technology in Green Buildings (ATiGB 2024)

Determine the Short Circuit cutting Time of Fuse Cut Out for Energy saving Amorphous Core Transformers

Bao Doan Thanh
Faculty of Engineering & Technology Quy Nhon University
140 An Duong Vuong, Quy Nhon, Binh Dinh, Vietnam
doanthanhbao@qnu.edu.vn
ORCID: https://orcid.org/0000-0002-9180-9862

***Abstract* — In this article, we use the finite element method (FEM) with Ansys Electromagnetics to imilate two Amorphous core transformers (ACTs) with a capacity of 400kVA and 1600kVA; working in rated modes and three phase short circuit (SC) on the low voltage winding (LVW). From there, the largest SC current can be determined; and the largest SC electromagnetic force (EMF) have an effect on the LVW and high voltage winding (HVW) of ACTs. At the same time, research and build and coordinate between the Ampere-second characteristics of the ACTs and the characteristics of the fuse cut out (FCO), thereby determining the correct SC cutting time of the ACTs. We determine the correct SC cut-off time to support the correct FCO selection, from which the ACTs will avoid the harmful effects of EMF that cause the winding ACTs to break. The results of this study help us determine the correct time to cut off the SC of the FCO to disconnect the ACTs from the high voltage grid. From there, protect against SC breakage and displacement of the ACTs's winding caused by SC EMF.**

Keywords— Ansys Electromagnetics, Short circuit, Electromagnetic Forces, Amorphous Core Transformers, Fuse cut out.

I. INTRODUCTION (*HEADING 1*)

Amorphous core transformers (ACTs) are used in countries around the world with the special feature of reducing no-load losses. ACTs is constructed from a 0.03mm ultra-thin steel core. In Vietnam, provincial power companies have installed ACTs on their local power grids. ACTs are more effective in reducing power losses than silicon steel core transformers currently in use [1-4].

The electromagnetic force (EMF) in the winding of the ACTs is developed between the current in the wingding and the induction flux in the winding sections and in the core. During the operation of the ground fault of the ACTs, the current in the winding and the induction flux increase greatly, and a large EMF is generated on the winding. Therefore, the mechanical structure of the winding and the fixed part must be designed to withstand this EMF. Therefore, it is necessary to accurately calculate the stress when short-circuited, which will significantly improve the size of the ACTs [5-8]. To calculate the EMF have an effect on the concentric coil under external SC conditions. One computational approach is to use the FEM, which results in 2D images of the stray the induction flux density and the average EMF, and then compares them with the classical analytical method. In addition, the works have calculated the EMF distribution when the low voltage short circuit (SC) fault occurs; generating mechanical forces have an effect on the high voltage winding (HVW) and low voltage winding (LVW) of the ACTs; The method used throughout is to use Anys 2D (FEM) software for time domain analysis, but it performs a very large mesh, so the results are not accurate [9-13].

In Ref [14], The authors used the FEM to analyze and calculate the force stress have an effect on the HVW and LVW of the 20MVA; 132/11.5 kV transformer in the case of a SC. The results are 2D images of the stray magnetic field density and electromagnetic force, which are compared with the classical analytical method. In addition, the effects of short circuit current (SCC) and asymmetrical force at different positions on the HVW and LVW of the transformer are also taken into account. In Ref [15-16] The FEM analyzed the effects of SCC in each part of the winding of the transformer using the method of combining magnetic and electric circuits. Using the FEM to imitate the transformer in the case of a test SC, the results of SCC, stray magnetic field and axial and radial FEM have an effect on the HVW and LVW in the case of a SC fault in part of the winding or the entire winding.

The authors [17-23], Following the above research works, the presentation of the calculation of radial and axial forces have an effect on the winding wire only stops at the average value. The work has not taken into account the force distribution and sometimes has not found the position with the greatest stress on the winding wire. It can be seen that the works of the authors have made efforts in calculating the EMF but are still limited in quantity; The works on ACTs have not received much attention from documents on scientific forums.

We see that, in reference works, there is no generalized analysis and assessment of SC cases; linear planning. We need: (1) – a model to evaluate the interaction between electric current and induction flux; EMF have an effect on the windings of many different ACTs capacities; (2) - we need to build a general Ampere-second characteristic, combining the current characteristics of the self-falling fuse FCO and the SCC characteristics of the ACTs. These essential research results help: (*) - choosing self-falling fuses to protect the ACTs from the harmful effects of EMF have an effect on the windings; (**) - manufacturing of ACTs' winding; and electric utilities that operate ACTs.

In this article, we use FEM with Ansys Electromagnetics to imilate two ACTs with different capacities [24]; working in rated modes and three-phase SC on the LVW. Therefrom, we define the largest SCC; and the largest SC EMF influence on the LVW and HVW, and at the same time check the limit of mechanical force generated to destroy the windings. Not only

that, research continues to develop the Ampere-second protection characteristic of fuse cut out (FCO), helping to determine the correct short-circuit cutting time of the ACTs. From there, technical recommendations are provided to help design, test and operate ACTs more completely.

II. SHORT CIRCUIT CURRENT AND ELECTROMAGNETIC FORCE

A. *Short circuit current (SCC)*

In case the transformer is working with the nominal primary voltage, if a SC occurs on the secondary side, the SCC will be very large. At this time, the entire nominal voltage is applied to the very small SC impedance of the transformer, so it is called an operating SC. The SCC is as follows [1, 7, 9]

$$i = I_{SC}\sqrt{2}\left[\sin(\omega t - \psi - \varphi_{SC}) + \sin(\psi + \varphi_{SC}).e^{-\frac{R_{SC}}{X_{SC}}\omega t}\right] \quad (1)$$

where:

- $I_{SC} = \frac{U_{Nominal}}{Z_{SC}}$ is SC current (A),

- $\varphi_{SC} = \text{arctg}\frac{X_{SC}}{R_{SC}}$, is the phase angle (rad),

- U_{Nom}: Nominal voltage (V)

- Z_{SC}: SC impedance (Ω) (Ω),

- X_n and R_n are respectively short-circuit resistance and reactance (Ω),

- t is the time (s),

- ψ: angle at the moment of SC (rad),

- ω is the angular frequency (rad/s).

B. *Electromagnetic force*

The interaction between active current (I_{AC}) and induction flux (B_{InF}) in the windings, creating F_{EMF} in the transformer windings. According to the Lorentz formula, we write the EMF relationship as [8,12,15,18]:

$$F_{EMF} = \int_L I_{AC}.B_{InF}\sin(\overrightarrow{I_{AC}}, \overrightarrow{B_{InF}})d\ell \quad (2)$$

Or:

$$d\vec{F}_{EMF} = \overrightarrow{B_{InF}} \times \overrightarrow{I_{AC}}d\ell = \overrightarrow{B_{InF}} \times \overrightarrow{J_{Ws}}.d\rho.d\ell \quad (3)$$

where:

- I_{AC} (A) and J_{Ws} (A/m^2) are the active and intensity of the current in the wingdings;

- B_{InF} (T) and F_{EMF} (N) are the induction flux and EMF;

- $d\rho$; $d\ell$ are the differential area and length of wingdings

III. AMORPHOUS CORE TRANSFORMERS

A. *The factor of amorphous core transformer (FACTs) 400kVA*

Fig. 1 shows an actual image of an ACTs with a capacity of 400kVA. All the detailed electrical coefficients of ACT are taken from the design of SANAKY in Hanoi; all the above factors are included in the entire simulation process of this research.

Fig. 1. ACTs - 400kVA

B. *Transformer simulation by design parameters*

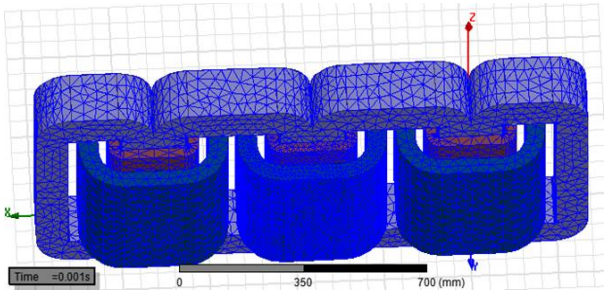

Fig. 2. ACTs model used in Ansys Maxwell 3D

The factors of this ACTs 400kVA 22/0.4kV are set up a very detailed; this process is completely based on FEM of Ansys Electromagnetics 2019; we carefully check the input quantities; analyze and perform the meshing model as shown in Fig 2. The working process of ACTs is designed using Maxwell Circuit Editor V19.02 circuit at Fig 3; ACTs works in the following cases: no load; rated load and short circuit fault cases; these processes are similar to real operations on the distribution grid.

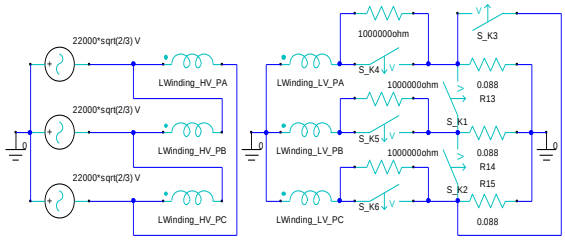

Fig. 3. The Transformer's Maxwell Circuit Editor

C. *Results of simulation about voltage and current values at full load of ACTs*

The simulation problem of ACTs is established in the time series; We set the simulation working mode option of ACTs ourselves; In this research, ACTs are set to no load and rated load mode with t = 100ms. The resulting sine wave form on these HVW and LVW are shown in Fig 4 and Fig 5 below:

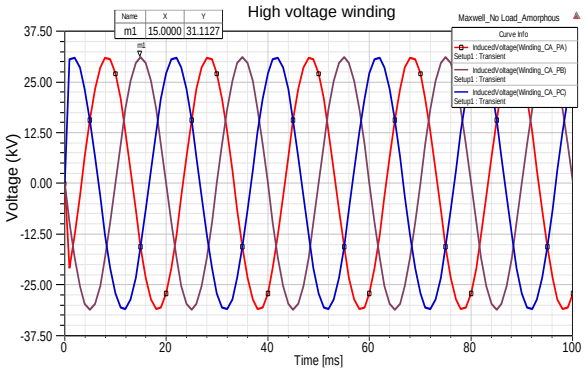

Fig. 4. Three-phase rated voltage in the HVW

In Fig. 4, Result of $31.11/\sqrt{2} = 21.99$kV is the rated phase voltage value on the HVW of FEM method; This value is collated to the calculated phase voltage value of 22kV of analytic method. The likewise, in Fig. 5, the rated phase voltage value on the LVW of FEM method is $309.2/\sqrt{2} = 218.6$V; It is collated to the calculated phase voltage value of 220V of analytic method.

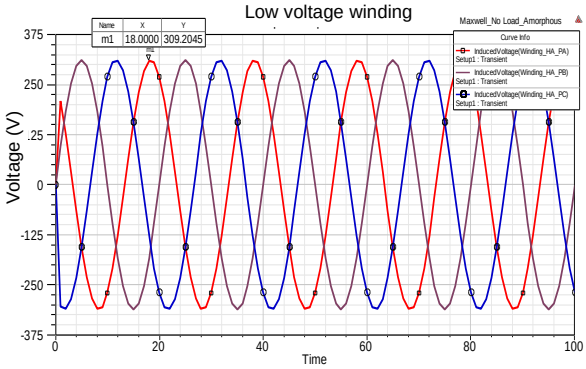

Fig. 5. Three-phase rated voltage in the LVW

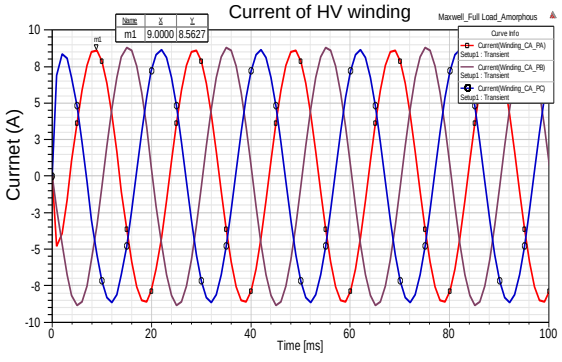

Fig. 6. Three- phase rated current in the HVW

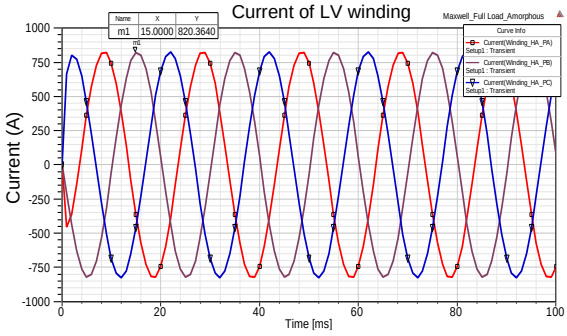

Fig. 7. Three- phase rated current in the LVW

In Fig. 6, Result of 6.06A is the rated phase current value of the HVW of FEM method; This value is collated to the calculated phase voltage value of 6.05A of analytic method. The likewise, Fig. 7, the rated phase current of LVW is 577.4A; It is collated to the calculated phase voltage value of 579.8A of analytic method.

At Table I, comparion of the currents and voltages between the analytic and FEM method.

TABLE I. COMPARATIVE TEST OF THE CURRENTS AND VOLTAGES BETWEEN THE ANALYTIC AND FEM METHOD

No.	Parameter of HV and LV winding		Calculation	Simulation	Error (%)
1	U_{rate} (V) - Rated phase voltage	HV	21990	22000	0.05
		LV	218,6	220	0.6
2	I_{rate} (A) - Rated phase current	HV	6,05	6,06	0.2
		LV	579,8	577,4	0.4

From the results of Table II, we see that simulation and calculation are nearly equal. Showing that the simulation results are an accurate method, we can then use the simulation for the next SC case.

D. Simulation results in short circuit mode of ACTs

Analysis of the SC mode is performed by closing key K on the circuit of Maxwell Circuit Editor V16.02 software, all this is in Fig. 3. We setup the SC on the LVW of the ACTs, then the result of the voltage of the LVW to value 0. The likewise, we have the following SCC results:

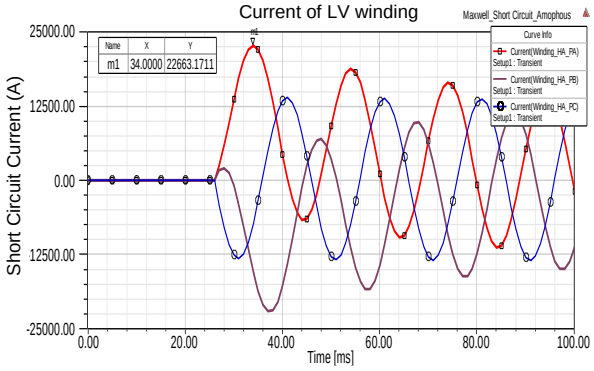

Fig. 8. SCC in the LVW

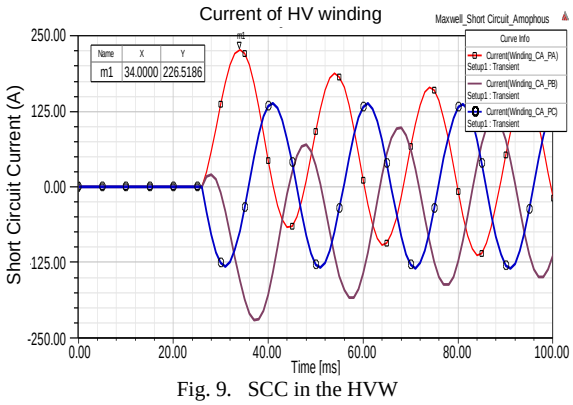

Fig. 9. SCC in the HVW

The results of the LVW and HVW SCC analysis are displayed in Fig. 8 and Fig. 9, displaying that: At t = 34 ms, the amplitude value of the largest SCC on LVW phase A, I_{LV_max} = 22663.2 A and that of HVW I_{HV_max} = 226.5 A;

Compared to the rated current amplitude, it is up to 27 times higher. Values are displayed in Table II.

TABLE II. LARGEST VALUE OF EMF ON HVW AND LVW

The winding	**Rated current amplitude (A)**	**Largest SCC amplitude (A)**	**Ratio**
LVW	$577,4\sqrt{2}$	22663,2	27,8
HVW	$6,06\sqrt{2}$	226,5	26,4

IV. RESULTS OF EMF HAVE AN EFFECT ON THE HVW AND LVW

A. Results of simulation Transformer 400kVA

The simulation and analysis results show the largest total EMF distribution on the HVW and LVW when the ACTs experiences a SC. These results are shown in the following figures.

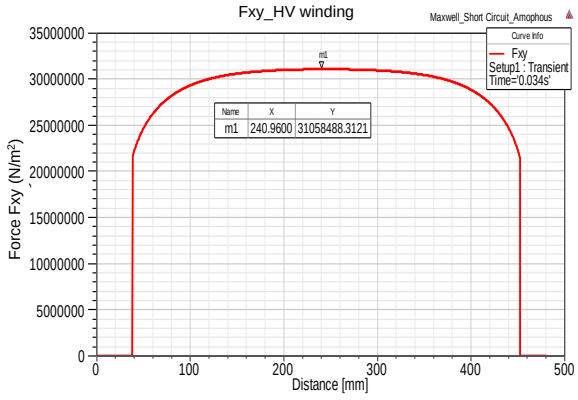

Fig. 10. Diagram of component forces Fxy of the HVW

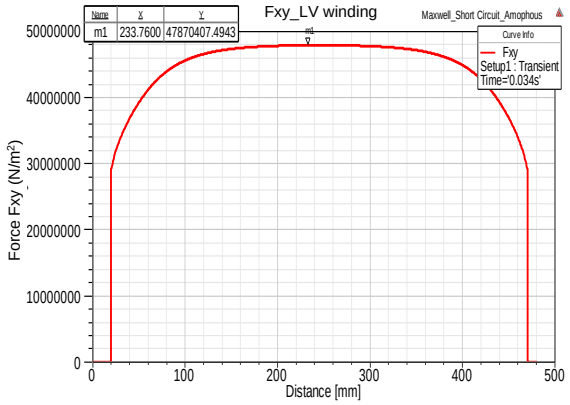

Fig. 11. Diagram of component forces Fxy of the LVW

Looking at the Fig. 10 and Fig. 11, the simulation results show the distribution of EMF according to the winding height; According to the winding height, we see that the EMF is largest in the middle of the winding and the EMF tends to decrease at the lower and upper ends of the winding. Regarding the direction of action, the direction of EMF on the two winding is opposite; The total EMF have an effect to pull LVW into the steel core but push HVW away from the steel core.

The largest value of total EMF on HVW and LVW is displayed in TABLE III.

TABLE III. LARGEST VALUE OF EMF ON HVW AND LVW

Total EMF F_{xymax} (N/m²)	**HVW**	**LVW**
F_{xymax}	3.106×10^7	4.787×10^7
Allowable stress limit: σ_{ASL}	5.10^7	
Comparing F_{xymax} with σ_{ASL}	$4.787\times10^7 < 5\times10^7$	

In Table III, the largest EMF is $F_{xymax} = 4.787\times10^7$ N/m² while the strain limit of windings $\sigma_{ASL} = 5\times10^7$ N/m² [9]. When the SCC value is 27 times greater than the nominal current, the largest EMF of the windings is close to the allowable limit value. However, if the SC time is extended longer, the functional preparation of the HVW and LVW may be disrupted.

B. Results of simulation Transformer 1600kVA

Similarly, based on simulation analysis on the FEM such as ACTs 400kVA. Research conducted for ACTs 1600kVA - 22/0.4kV; connect the Δ/Y. The results of analyzing the SCC value and EMF distribution on the HVW and LVW are as follows:

TABLE IV. COMPARATIVE TEST THE ANALYTIC AND FEM METHOD OF THE CURRENTS AND VOLTAGES

No.	**Parameter of HVW and LVW**		**Calculation**	**Simulation**	**Error (%)**
1	U (V) – Rated phase voltage	HV	22000	22005	0.02
		LV	231	220	4.9
2	I_{rate} (A) - Rated phase current	HV	24.24	23.49	3.1
		LV	2309.40	2315.17	0.2
3	Fault SC impulse current (A)	HV	1102.8	1109.4	0.6
		LV	111 090	111 076	0.01

The results of voltage, nonimal current and SCC on HVW and LVW between preliminary calculation and simulation, are compared and displayed in TABLE IV.

Similarly, continuing to analyze the EMF gives the results in Fig. 12 and Fig. 13.

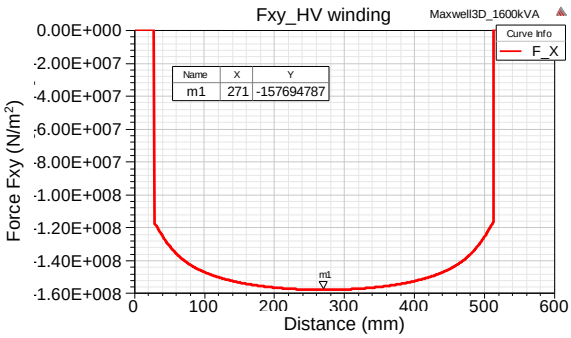

Fig. 12. Diagram of component forces F_{xy} of the HVW

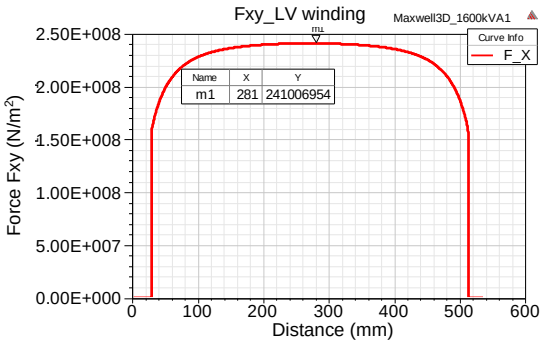

Fig. 13. Diagram of component forces F_{xy} of the LVW

The largest value of total EMF on HVW and LVW is displayed in TABLE V.

TABLE V. LARGEST VALUES OF EMF ON HVW AND LVW

Total EMF F_{xymax} (N/m^2)	**HVW**	**LVW**
F_{xymax}	15.76×10^7	24.10×10^7
Allowable stress limit: σ_{ASL}	5.10^7	
Comparing F_{xymax} with σ_{ASL}	$5\times10^7 < 24.10\times10^7$	

In Table V, the largest EMF is $F_{xymax} = 24.10\times10^7$ N/m^2 while the strain limit of windings $\sigma_{ASL} = 5\times10^7$ N/m^2 [9]. So, the largest EMF is much larger than the strain limit of windings.

V. SHORT-CIRCUIT CUTTING TIME CHARACTERISTIC OF THE FCO AND ACTS

A. *Cutting characteristics of ACTs 400kVA*

The FCO is installed in series with the three-phase 22kV high-voltage power grid to provide large overload and SC protection for the ACTs. With the Ampere-second SC characteristics of the ACTs, we combine with the melting characteristics of the K [25]; to determine the cutting time of the FCO when a SC of the ACTs occurs. From Fig. 14, consider the following two typical cases:

At Fig. 14, cutting characteristics of ACTs 400kVA: For ACTs 400kVA (22/0.4kV) - fuse type 15K is used.

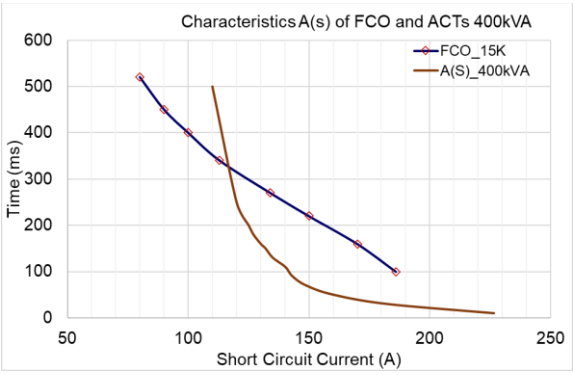

Fig. 14. Characteristics of ACTs 400kVA

At Fig. 14, when the A(s) characteristic in the SCC region is large, the time is less than 300ms, it does not touch the melting characteristic of FCO_15K. At that time, the wire had not melted, the FCO had not blown, meaning the ACTs had not been SC and was still connected to the high-voltage power source. But when the time increases to t = 320ms, the A(s) characteristic touches the FCO_15K characteristic, at which time FCO breaks the fuse wire, the ACTs is disconnected from the high-voltage grid. Thanks to that, the SC protection for the ACTs is not damaged at this time.

B. *Cutting characteristics of ACTs 1600kVA*

At Fig. 15, cutting characteristics of ACTs 1600kVA: For ACTs 1600kVA (22/0.4kV) - fuse type 65K is used.

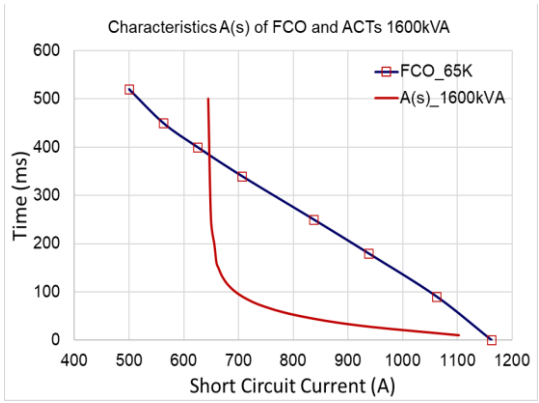

Fig. 15. Characteristics of ACTs 1600kVA

Similarly, looking at Fig. 15, when the ACTs is SCC for a short time of less than 380ms, the FCO wire does not have enough time to break the fuse wire. Characteristic A(s) intersects characteristic FCO_65K at the time t =380ms, at this time the FCO fuse wire breaks, the ACTs is disconnected from the high voltage grid. Thanks to that, the SC protection for the ACTs is not damaged at this time.

VI. CONCLUSIONS

The research employed FEM with Ansys Electromagnetics to imilate operating condition modes of ACTs with capacity of 400kVA and 1600kVA, voltage 22/0.4kV. The results for FEM method and analytic method about nonimal voltage, nonimal current, and SCC were tested for comparison. The research found out that the largest SCC on HVW and LVW is 27 times higher than the nonimal current. Therefore, found out the largest EMF distribution have an effect on the phases of the HVW and LVW.

The successful contribution of this study is to build the relationship between short-circuit current and time. The article has combined the FCO characteristics and the short-circuit A(s) characteristics of the ACTs, thereby building the typical short-circuit cut-off time characteristics of two ACTs with capacities of 400kVA and 1600kVA. In addition, from the results of this research we can build short-circuit cut-off time characteristics for many remaining ACTs capacities. The results of this research help operating engineers and ACTs manufacturers determine the correct FCO of SC time to disconnect the ACTs from the high-voltage grid. From there, protect against short-circuit breakage and winding displacement of the ACTs caused by short-circuit electromagnetic forces.

REFERENCES

[1] Bao Doan Thanh - Chi Phi Do - Huynh Duc Hoan - Le Thai Hiep, "Analysis of Current and Electromagnetic Force Acting on Winding in Cases of Short Circuits of Amorphous Transformer," 2023 8th Int. Sci. Conf. Appl. New Technol. Green Build. ATiGB 2023, no. November, pp. 201–208, 2023, doi: 10.1109/ATiGB59969.2023.10364484.

[2] L. Roginskaya, Z. Yalalova, A. Gorbunov, and J. Rakhmanova, "Features of amorphous steel magnetic cores for transformers operating at mains frequency," Proc. - ICOECS 2020 2020 Int. Conf.

Electrotech. Complexes Syst., pp. 12–16, 2020, doi: 10.1109/ICOECS50468.2020.9278451.

[3] M. E. M. Nazmunnahar M, S. Simizu, P. R. Ohodnicki, S. Bhattacharya, “Finite-Element Analysis Modeling of High-Frequency Single-Phase Transformers Enabled by Metal Amorphous Nanocomposites and Calculation of Leakage Inductance for Different Winding Topologies,” IEEE Trans. Magn., vol. 55, no. 7, pp. 1–11, 2019, doi: 10.1109/TMAG.2019.2904007.

[4] S. Z. Deren Li, Liang Zhang, Guangmin Li, Zhichao Lu, “Reducing the core loss of amorphous cores for distribution transformers,” Prog. Nat. Sci. Mater. Int., vol. 22, no. 3, pp. 244–249, 2012, doi: 10.1016/j.pnsc.2012.04.005.

[5] C. Hsu, C. Lee, Y. Chang, F. Lin, C. Fu, and J. Lin, “Effect of Magnetostriction on the Core Loss, Noise, and Vibration of Fluxgate Sensor Composed of Amorphous Materials,” IEEE Trans. Magn., vol. 49, no. 7, pp. 3862–3865, 2013.

[6] Y. Wang et al., “Development of a 630 kVA Three-Phase HTS Transformer With Amorphous Alloy Cores,” IEEE Trans. Appl. Supercond., vol. 17, no. 2, pp. 2051–2054, Jun. 2007, doi: 10.1109/TASC.2007.898162.

[7] M. Mouhamad, C. Elleau, F. Mazaleyrat, C. Guillaume, and B. Jarry, “Short-Circuit Withstand Tests of Metglas 2605SA1-Based,” IEEE Trans. Magn., vol. 47, no. 10, pp. 4489–4492, 2011, doi: 10.1109/TMAG.2011.2155632.

[8] Hyun-mo Ahn - Yeon-ho Oh and - Joong-kyoung Kim - Jae-sung Song - Sung-chin Hahn, “Experimental Verification and Finite Element Analysis of Short-Circuit Electromagnetic Force for Dry-Type Transformer,” IEEE Trans. Magn., vol. 48, no. 2, p. 819--822, February, 2012.

[9] Marcel Dekler, “Transformer_Engineering_-_Design_and_Practice - Chapter 6: Short Circuit Stresses and Strength,” no. year 2000, pp. 231–275.

[10] G. qiang Z. Haifeng Zhong, WenhaoNiu, Tao Lin, Dong Han, “The Analysis of Short-Circuit Withstanding Ability for A 800KVA/10KV Shell-Form Power Transformer with Amorphous Alloy Cores,” 2012 IEEE Int. Conf. Electr. Distrib., no. 2161–7481, pp. 1–5, 2012, doi: 10.1109/CICED.2012.6508689.

[11] T. Steinmetz, B. Cranganu-Cretu, and J. Smajic, “Investigations of no-load and load losses in amorphous core dry-type transformers,” XIX Int. Conf. Electr. Mach. - ICEM 2010, pp. 1–6, Sep. 2010, doi: 10.1109/ICELMACH.2010.5608162.

[12] M. B. B. Sharifan, R. Esmaeilzadeh, M. Farrokhifar, J. Faiz, M. Ghadimi, and G. Ahrabian, “Computation of a single-phase shell-type transformer windings forces caused by inrush and short-circuit currents,” J. Comput. Sci., vol. 4, no. 1, pp. 51–58, 2008, doi: 10.3844/jcssp.2008.51.58.

[13] S. Hajiaghasi and K. Abbaszadeh, “Analysis of Electromagnetic Forces in Distribution Transformers Under Various Internal Short-Circuit Faults,” CIRED Reg. - Iran, Tehran, vol. 13–14, pp. 1–9, 2013.

[14] A. Ahmad, I. Javed, and W. Nazar, “Short Circuit Stress Calculation in Power Transformer Using Finite Element Method on High Voltage Winding Displaced Vertically,” International Journal of Emerging Technology and Advanced Engineering, ijetae.com, vol. 3, no. 11, 2013.

[15] G. B. Kumbhar and S. V. Kulkarni, “Analysis of Short-Circuit Performance of Split - Winding Transformer Using Coupled Field-Circuit Approach,” IEEE transactions on power delivery, vol. 22, no. 2, april 2007, pp.936-943.

[16] K. Dawood, G. Komurgoz and F. Isik, "Computation of the Axial and Radial forces in the Windings of the Power Transformer," 2019 4th International Conference on Power Electronics and their Applications (ICPEA), Elazig, Turkey, 2019, pp. 1-6, doi: 10.1109/ICPEA1.2019.8911132.

[17] Y. G. and S. L. Y. Zhai, R. Zhu, Q. Li, X. Wang, “Simulation Research on Electrodynamic Force and Deformation of Transformer Windings under Short-circuit Condition,” IEEE Int. Conf. High Volt. Eng. Appl., pp. 1–4, 2022, doi: 10.1109/ICHVE53725.2022.9961358.

[18] Y. Zhao, T. Wen, Y. Li, H. Ni, Q. Zhang, and W. Chen, “A FEM-based simulation of electromagnetic forces on transformer windings under short-circuit,” 2018 IEEE Int. Power Modul. High Volt. Conf. IPMHVC 2018, pp. 425–429, 2018, doi: 10.1109/IPMHVC.2018.8936726.

[19] Q. Z. Mingkai Jin, Tao Wen, Weijiang Chen, Yi Zhao, Jie Wu, Xingwang Wu, “Influence of Frequency Components of Short-Circuit Electromagnetic Force on Vibration Characteristics of Power Transformer Windings,” 2022 IEEE Int. Conf. High Volt. Eng. Appl., pp. 01–04, 2022, doi: doi: 10.1109/ICHVE53725.2022.9961671.

[20] K. Dawood and G. Komurgoz, “Investigating effect of Electromagnetic Force on Sandwich Winding Transformer using Finite Element Analysis,” 2021 28th Int. Work. Electr. Drives Improv. Reliab. Electr. Drives, IWED 2021 - Proc., pp. 1–5, 2021, doi: 10.1109/IWED52055.2021.9376371.

[21] J. U. Kothavade and P. Kundu, “Investigation of Electromagnetic Forces in Converter Transformer,” Proc. 2021 IEEE 2nd Int. Conf. Smart Technol. Power, Energy Control. STPEC 2021, pp. 1–6, 2021, doi: 10.1109/STPEC52385.2021.9718676.

[22] Chen Yi Zhao; Weijiang Chen; Mingkai Jin; Tao Wen; Jiyin Xue; Qiaogen Zhang; Ming, “Short-Circuit Electromagnetic Force Distribution Characteristics in Transformer Winding Transposition Structures,” IEEE Trans. Magn., vol. 56, no. 12, pp. 1–8, 2020, doi: 10.1109/TMAG.2020.3028832.

[23] Bao Doan Thanh - Do Chi Phi, “Calculation of the Magnetic Field and Inrush Current in a Three-phase Transformer,” Proc. 2020 Appl. New Technol. Green Build. ATiGB 2020, no. March, pp. 94–99, 2020, doi: 10.1109/ATiGB50996.2021.9423111.

[24] ANSYS Inc, “ANSYS Maxwell 3D V19,” ansysinfo@ansys.com, vol. 19, no. REV5.0, pp. 1–1011, 2016.

[25] Nguyễn Hoàng Việt, “Bảo vệ rơle và Tự động hoá trong hệ thống điện,” NXB Đại học Quốc Gia Hồ Chí Minh, pp. 1–492, 2005.